Steric and not structure-specific factors dictate the endocytic mechanism of glycosylphosphatidylinositol-anchored proteins

Pinkesh Bhagatji,[1] Rania Leventis,[1] Jonathan Comeau,[2] Mohammad Refaei,[1] and John R. Silvius[1]

[1]Department of Biochemistry, McGill University, Montreal, Quebec H3G 1Y6, Canada
[2]Department of Chemistry, St. Francis Xavier University, Antigonish, Nova Scotia B2G 2W5, Canada

Diverse glycosylphosphatidylinositol (GPI)-anchored proteins enter mammalian cells via the clathrin- and dynamin-independent, Arf1-regulated GPI-enriched early endosomal compartment/clathrin-independent carrier endocytic pathway. To characterize the determinants of GPI protein targeting to this pathway, we have used fluorescence microscopic analyses to compare the internalization of artificial lipid-anchored proteins, endogenous membrane proteins, and membrane lipid markers in Chinese hamster ovary cells. Soluble proteins, anchored to cell-inserted saturated or unsaturated phosphatidylethanolamine (PE)-polyethyleneglycols (PEGs), closely resemble the GPI-anchored folate receptor but differ markedly from the transferrin receptor, membrane lipid markers, and even protein-free PE-PEGs, both in their distribution in peripheral endocytic vesicles and in the manner in which their endocytic uptake responds to manipulations of cellular Arf1 or dynamin activity. These findings suggest that the distinctive endocytic targeting of GPI proteins requires neither biospecific recognition of their GPI anchors nor affinity for ordered-lipid microdomains but is determined by a more fundamental property, the steric bulk of the lipid-anchored protein.

Introduction

Mammalian cells exploit a variety of endocytic pathways to internalize components of the plasma membrane. The classical clathrin-dependent pathway has been shown to be complemented by multiple clathrin-independent pathways that mediate the endocytosis of particular complements of plasma membrane proteins and other endocytic cargo (Skretting et al., 1999; Sabharanjak et al., 2002; Guha et al., 2003; Pelkmans et al., 2004; Bonazzi et al., 2005; Cheng et al., 2006). However, many aspects of the diversity, the cargo specificity, and the molecular mechanisms of clathrin-independent endocytic pathways remain to be clarified (Mayor and Riezman, 2004; Kirkham and Parton, 2005; Mayor and Pagano, 2007; Sandvig et al., 2008; Donaldson et al., 2009).

Glycosylphosphatidylinositol (GPI)-anchored proteins constitute one class of membrane proteins that are internalized mainly by clathrin-independent processes in various cell types. When clustered by extracellular agents, GPI proteins can be internalized via caveolae (Mayor et al., 1994). In contrast, in the absence of clustering agents, diverse GPI-anchored proteins are internalized primarily by a distinct endocytic process that has been termed the GPI-enriched early endosomal compartment (GEEC) or clathrin-independent carrier (CLIC) pathway (Sabharanjak et al., 2002; Gauthier et al., 2005; Kirkham et al., 2005). This pathway is independent of clathrin, dynamin, and caveolin, is regulated by the small G proteins Arf1 and cdc42, and is highly sensitive to perturbation of actin polymerization (Kirkham et al., 2005; Chadda et al., 2007; Kumari and Mayor, 2008). Certain bacterial toxins that are endocytosed in a GPI protein–dependent manner, such as aerolysin and *Helicobacter pylori* VacA, as well as a substantial fraction of pinocytosed fluid-phase markers are also internalized via the GEEC/CLIC pathway (Ricci

Correspondence to John R. Silvius: john.silvius@mcgill.ca

Abbreviations used in this paper: CLIC, clathrin-independent carrier; DCC, dicyclohexylcarbodiimide; DHFR, dihydrofolate reductase; DIEA, diisopropylethylamine; DMF, dimethylformamide; GEEC, GPI-enriched early endosomal compartment; GPI, glycosylphosphatidylinositol; NHS, *N*-hydroxysuccinimide; PE, phosphatidylethanolamine; PEG, polyethyleneglycol; shRNA, small hairpin RNA; TFA, trifluoroacetic acid; Trt, trityl.

The Rockefeller University Press $30.00
J. Cell Biol. Vol. 186 No. 4 615–628
www.jcb.org/cgi/doi/10.1083/jcb.200903102

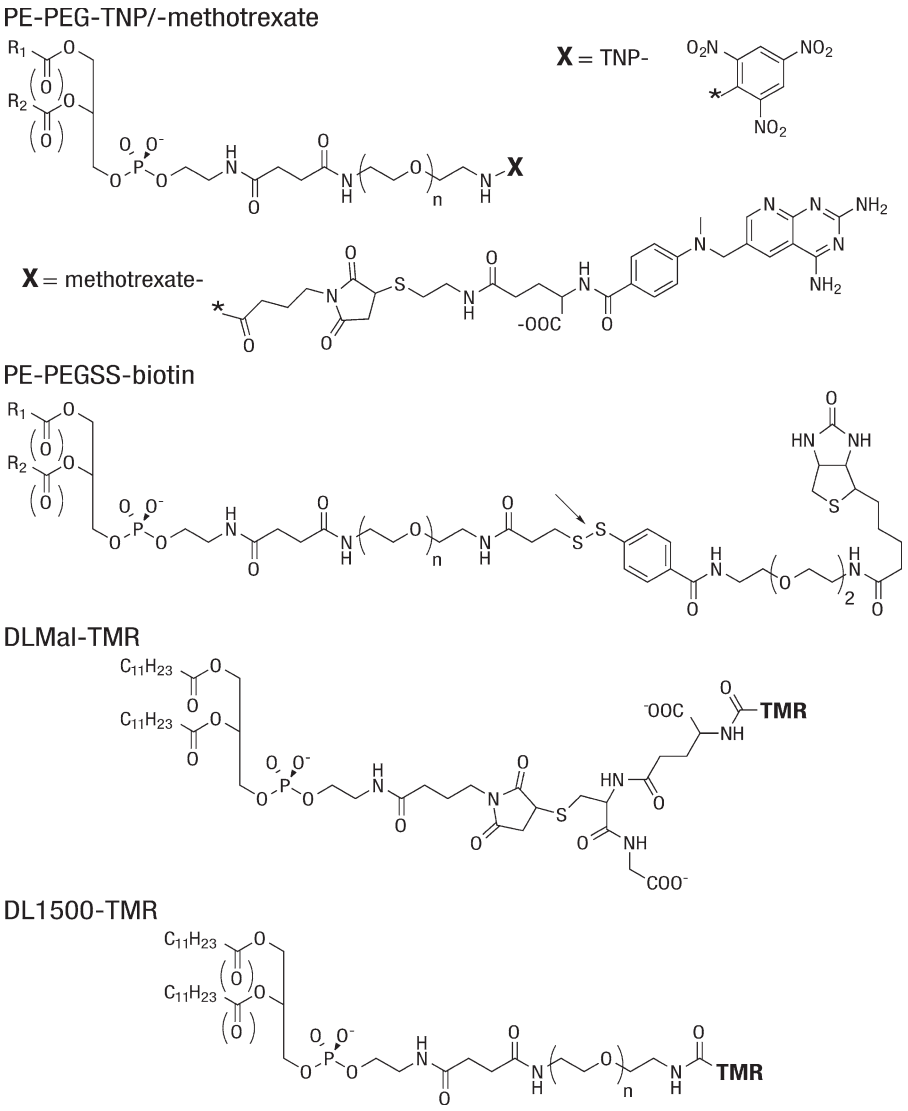

Figure 1. **Structures of PE-PEG ligand conjugates and fluorescent lipid markers.** Structures of the PE-PEG ligand conjugates used in this study (R_1 and R_2 are alkyl chains with varying structures, as indicated in the text; asterisks indicate sites of linkage of group X to the PE-PEG anchor), the bulk lipid marker DLMal-TMR, and the fluorescent PE-PEG species DL1500-TMR are shown. Anti-DNP antibody binds strongly to the TNP group of PE-PEG-TNP but can be displaced at acidic pH in the presence of the competing ligand ε–DNP-lysine. Streptavidin binds tightly to the biotinyl residue of PE-PEGSS-biotin but can be released by cleavage of the disulfide bond (arrow) in thiol-containing media. *E. coli* DHFR binds tightly to PE-PEG-methotrexate but can be displaced by free methotrexate at neutral pH.

et al., 2000; Fivaz et al., 2002; Gauthier et al., 2005). Some transmembrane proteins that exhibit clathrin- and caveolin-independent endocytosis are found in GPI protein–containing, Arf6-associated peripheral endocytic structures that may be related to GEECs (Naslavsky et al., 2004; Barr et al., 2008; Eyster et al., 2009), although some other transmembrane proteins such as interleukin-2 receptor enter cells by apparently distinct clathrin/caveolin-independent pathways (Lamaze et al., 2001; Sabharanjak et al., 2002). However, at present, GPI proteins constitute the best-characterized endogenous membrane cargo for the GEEC/CLIC pathway.

The mechanism or mechanisms by which GPI proteins are internalized by the GEEC/CLIC pathway without showing significant parallel uptake via, for example, the clathrin-mediated endocytic pathway remain unclear. This question is of particular interest given that GPI proteins, lacking cytoplasmic domains, cannot directly engage intracellular elements of the cellular endocytic machinery. In principle, elements of the GPI anchor could bind to a common, as yet unidentified transmembrane adapter protein that recruits GPI proteins into the GEEC/CLIC pathway. Alternatively, the long-chain saturated lipid anchors found in many GPI proteins could direct the distinctive endocytic routing of these proteins by promoting their association with ordered-lipid microdomains or nanoclusters (Sharma et al., 2002, 2004; Chadda et al., 2007). Assessment of such possibilities is complicated by the relative paucity of approaches available to modify the organization and interactions of GPI proteins in cell membranes and by the highly pleiotropic effects of the approaches available (e.g., perturbation of cortical actin organization or of membrane cholesterol levels).

As an alternative approach to clarify the structural and physical bases for endocytosis of GPI proteins via the GEEC/CLIC pathway, we have investigated the manner in which proteins tethered to artificial phosphatidylethanolamine (PE)-polyethyleneglycol (PEG) anchors with different structures are internalized from the plasma membrane in CHO cells. We find that PE-PEG–anchored proteins are internalized in a manner that closely parallels that observed for GPI-anchored proteins, independently of both the identity of the artificially anchored protein and the physical properties of the PE-PEG anchor, but with a clear requirement for the steric bulk that the anchored protein contributes.

Results

As we have demonstrated previously for Jurkat and 3T3-L1 cells (Wang et al., 2005), PE-PEG protein conjugates with long acyl chains can be introduced into mammalian cell membranes by first incorporating into the cells a PE-PEG (ligand) anchor and then binding to the incorporated anchor molecules a protein that associates tightly with the tethered ligand. To facilitate investigation of the endocytic trafficking of these species, we developed three novel classes of PE-PEG ligand compounds (structures shown in Fig. 1) that strongly bind appropriate fluorescent proteins (anti-DNP antibody, streptavidin, or *Escherichia coli* dihydrofolate reductase [DHFR]) in physiological media but that also allow efficient removal of surface-bound proteins under appropriate conditions, allowing internalized PE-PEG protein complexes to be visualized selectively. For this study, we used FRαTb-1 cells, a CHO cell line that stably expresses the human transferrin and GPI-linked folate receptors and in which the GEEC/CLIC endocytic pathway has been particularly well characterized (Sabharanjak et al., 2002; Chadda et al., 2007; Kumari and Mayor, 2008). Cells incubated with fluorescent anti-DNP antibody, streptavidin, or DHFR without prior treatment with the relevant PE-PEG ligand anchor showed no significant fluorescent labeling above background levels (unpublished data), which is consistent with previous results (Wang et al., 2005). The fluorescent proteins bound to cells incorporating the appropriate PE-PEG ligand species were not detectably depleted from cell surfaces by repeated washing in mildly acidified medium, pH ≥ 5.0, indicating that the binding is not reversed by exposure to pH values typical of those encountered in endosomal compartments.

To examine the intracellular localization of artificially lipid-anchored proteins at early stages after endocytosis, cells incorporating PE-PEG ligand anchors were incubated for short times at 37°C with the appropriate fluorescent protein (and a second endocytic marker as indicated), rapidly chilled, stripped of uninternalized material in the cold, and then fixed and examined by fluorescence microscopy. As illustrated in Figs. 2 and 3, cells incorporating a long-chain saturated (di16:0) PE-PEG-TNP anchor and incubated for 10 min at 37°C with anti-DNP antibody show internalized lipid-anchored antibody both in a large central compartment, which is colabeled by simultaneously internalized transferrin and which has previously been identified as the recycling endosome (Dunn et al., 1989), and in small peripheral vesicles. The delivery of the lipid-anchored antibody to recycling endosomes resembles the behavior observed previously in CHO cells for GPI-anchored proteins and for artificial phospholipid-anchored GFP conjugates inserted into the cell surface (Mayor et al., 1998; Fivaz et al., 2002; Sabharanjak et al., 2002; Kalia et al., 2006; Paulick et al., 2007).

In contrast to their strong colocalization in central endosomal structures, transferrin and lipid-anchored anti-DNP antibody show markedly different distributions in the cell periphery (Figs. 2 and 3), where the lipid-anchored antibody and transferrin are found in largely divergent populations of early endocytic vesicles (Fig. 3, A–C). Under the same conditions, fluorescent-labeled folate, which is internalized as a complex with the GPI-anchored folate receptor, also appears in peripheral endocytic vesicles that are largely distinct from those labeled by simultaneously internalized transferrin (Fig. 3, D–F), as reported previously (Sabharanjak et al., 2002). In contrast, cells pretreated to incorporate di16:0PE-PEG-TNP and then coincubated with fluorescent anti-DNP antibody and folate show strong colocalization of the two markers in peripheral endocytic vesicles (Fig. 3, G–I). Low temperature treatment, like that used in this study to arrest endocytosis while removing surface-bound fluorescent markers, has been shown to lead to some fragmentation of GEEC/CLIC structures, which exist as larger tubulovesicular entities at 37°C (Sabharanjak et al., 2002; Kirkham et al., 2005; Lundmark et al., 2008). However, as the present and previous findings illustrate, this fragmentation does not lead to a mixing of markers endocytosed by different pathways.

The conditions used for the aforementioned experiments (10-min incubation of cells with endocytic markers at 37°C) were chosen to give optimal fluorescence labeling of peripheral endocytic structures without the need to prebind the endocytic ligands in the cold, thereby avoiding potential perturbations in membrane organization induced by exposing cells to low temperatures before initiating marker uptake. However, parallel

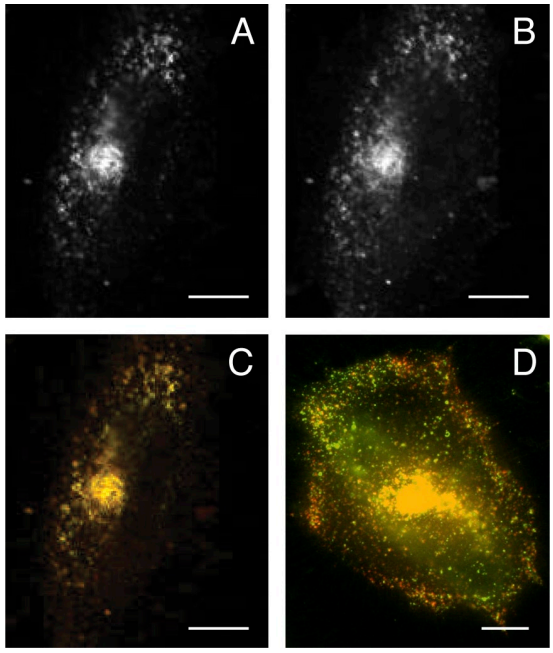

Figure 2. **Internalized anti-DNP antibody bound to a di16:0PEG anchor colocalizes with internalized transferrin in a central endosomal compartment but not in the cell periphery.** Cells pretreated to incorporate di16:0PEG-TNP were incubated for 10 min at 37°C with Alexa Fluor 488–labeled anti-DNP antibody and Alexa Fluor 555–transferrin and then rapidly chilled, stripped of surface-bound labels, and fixed before microscopic examination as described in Materials and methods. (A–C) Confocal images of the distribution of transferrin (A) and lipid-anchored anti-DNP antibody (B; C shows the merged image) show a strong coincidence of fluorescence labeling in the central region of the cell. The images shown in A and B were acquired under conditions in which the fluorescence intensity in the central region of the cell was not saturated and in which the peripheral region accordingly shows only weak fluorescence. (D) Wide-field microscopic image (with central fluorescence shown at saturating levels to reveal peripheral structures) illustrating the divergent distributions of lipid-anchored antibody (green) and transferrin (red) at the cell periphery. Bars, 10 µm.

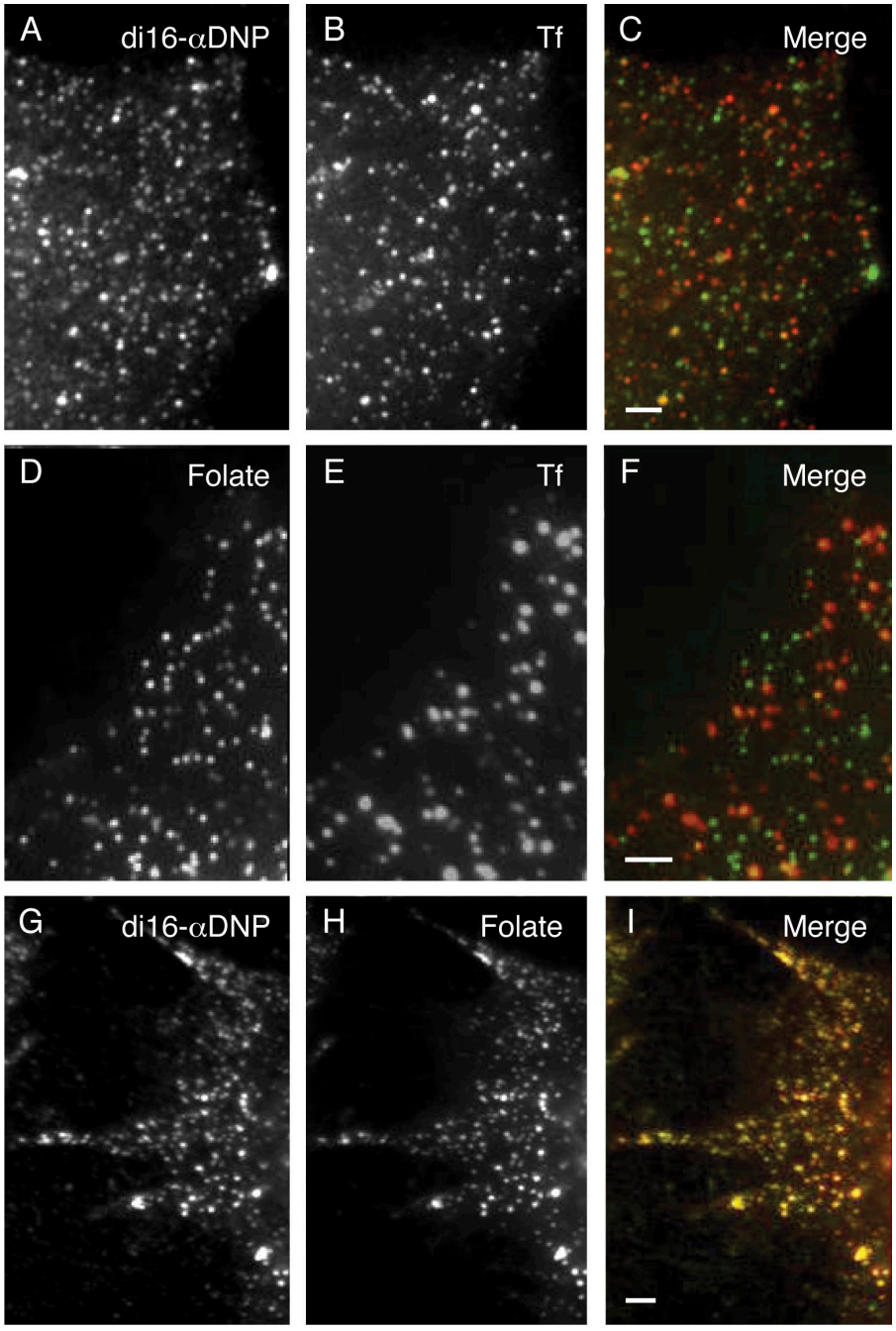

Figure 3. **Anti-DNP antibody bound to a di16:0PEG lipid anchor is internalized into peripheral endocytic structures that are largely distinct from transferrin-containing vesicles but that contain the GPI-linked folate receptor.** Cells pretreated to incorporate di16:0PE-PEG-TNP were incubated with the indicated pairs of endocytic markers for 10 min at 37°C and then rapidly chilled, stripped of surface-bound fluorescent labels, and fixed before microscopic observation as described in Materials and methods. (A–C) Cells coincubated with Alexa Fluor 488–anti-DNP antibody (green in merged image) and Alexa Fluor 555–transferrin (Tf). (D–F) Cells coincubated with fluorescein-labeled folate (green in merged image) and Alexa Fluor 555–transferrin. (G–I) Cells coincubated with Alexa Fluor 488–anti-DNP antibody (green in merged image) and rhodamine-labeled folate. Bars, 2 μm.

experiments in which cells were allowed to bind fluorescent endocytic markers at 0°C for 15 min and then warmed to 37°C for 3 min gave results quantitatively comparable with those illustrated in Fig. 3 (not depicted). Sabharanjak et al. (2002) have similarly reported that transferrin and folate receptor show a comparably high degree of segregation in peripheral endocytic vesicles in cells incubated at 37°C with the two endocytic markers for times ranging from 2 to 20 min.

Quantitative image analysis, performed as described in Materials and methods, confirmed that the distribution of di16:0PE-PEG–anti-DNP in peripheral endocytic vesicles closely resembles that of folate receptor (internalized via the GEEC/CLIC pathway) and differs strongly from that of labeled transferrin (internalized via clathrin-coated pits). As shown in Fig. 4 A, the degree of colocalization of di16:0PE-PEG–anti-DNP and folate in peripheral vesicles in the aforementioned experiments is comparable with that measured for fluorescein- and rhodamine-labeled folate in cells coincubated with these latter two ligands. In contrast, di16:0PE-PEG–anti-DNP and folate show comparably low degrees of colocalization with simultaneously endocytosed transferrin in peripheral vesicles.

To confirm that the early endocytic routing of PE-PEG–anchored anti-DNP antibody complexes is not determined specifically by the nature of the tethered protein, we also examined the endocytosis of streptavidin bound to cell-incorporated di16:0PE-PEGSS-biotin (structure shown in Fig. 1). As

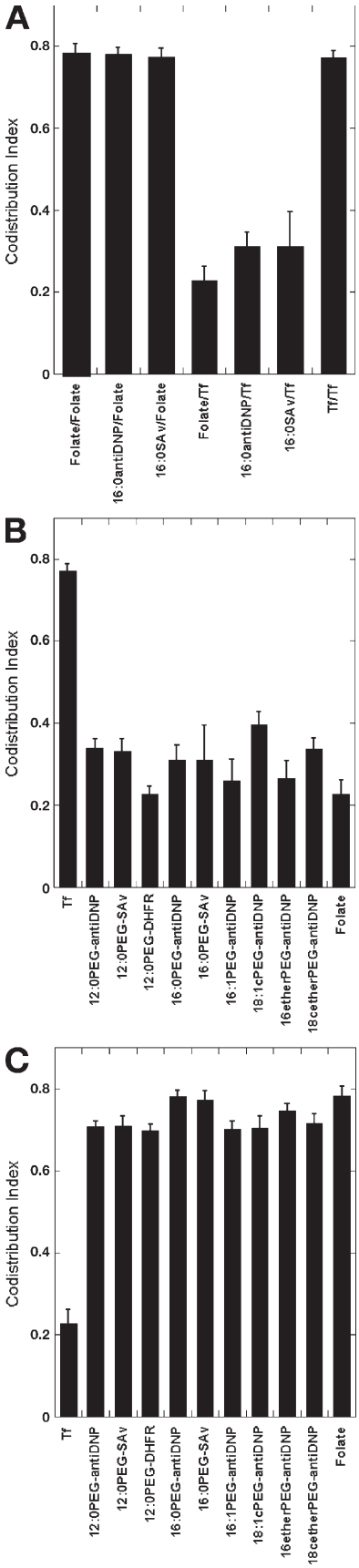

Figure 4. **Quantitative analysis of colocalization of di16:0PE-PEG–anchored proteins with transferrin and folate in endocytic vesicles.** (A) Cells incorporating di16:0PE-PEG-TNP or di16:0PE-PEGSS-biotin were coincubated with the indicated pairs of fluorescent markers (SAv, streptavidin; Tf, transferrin) for 10 min at 37°C, and then the extent of colocalization of the two markers in peripheral endocytic structures was determined by microscopy after removal of surface-bound markers and cell fixation (for further details, see Materials and methods). Data labeled folate/folate and Tf/Tf represent the values of the co-distribution index in peripheral endocytic vesicles measured for cells coincubated with fluorescein- and rhodamine-labeled folate or with Alexa Fluor 488– and Alexa Fluor 555–labeled transferrin, respectively, and indicate the value of the co-distribution index measured for species internalized in an identical manner. (B and C) Cells incorporating PE-PEG-TNP, PE-PEGSS-biotin or PE-PEG-methotrexate species with the indicated acyl or alkyl chains were incubated with labeled anti-DNP antibody, streptavidin, or DHFR, as appropriate, together with labeled transferrin (B) or folate (C), and the extent of colocalization of the two markers in peripheral vesicles was determined as described for A. Values plotted in A–C represent the mean (±SEM) of determinations for 30–60 separate fields (all representing distinct cells) in three to five independent experiments.

illustrated in Fig. 5 (A–C) and as quantified in Fig. 4 A, cells allowed to endocytose di16:0PE-PEG–anchored streptavidin together with labeled transferrin show only a low degree of colocalization of the two markers in peripheral vesicles, which is similar to the low degree of colocalization observed between internalized transferrin and folate under the same conditions. In contrast, internalized di16:0PE-PEG–streptavidin shows a high degree of colocalization with simultaneously internalized folate in peripheral endocytic structures, which is quantitatively comparable with that observed in cells coincubated with fluorescein- and rhodamine-labeled folate (Figs. 4 A and 5, D–F). These results qualitatively and quantitatively resemble the aforementioned results for di16:0PE-PEG–anchored anti-DNP antibody, indicating that the specific nature of the protein moiety does not determine the preferential internalization of PE-PEG protein conjugates into peripheral vesicles containing the folate receptor as opposed to vesicles containing the transferrin receptor. Given the low net charge exhibited by streptavidin in particular at neutral pH (estimated as −0.8 unit charges per streptavidin molecule at pH 7.2; Leckband et al., 1994), it appears moreover that electrostatic repulsions between a PE-PEG–anchored protein and other membrane proteins do not play an important role in determining the early endocytic routing of the PE-PEG–tethered species.

Further experiments showed that the early endocytic routing of PE-PEG protein conjugates is not substantially affected by varying the length or the degree of unsaturation of the hydrocarbon chains of the PE-PEG anchor. As illustrated in Fig. 6 and as summarized quantitatively in Fig. 4 (B and C), anti-DNP antibody or streptavidin anchored to cells via short-chain saturated (di12:0) or diunsaturated (di16:1 or di18:1) PE-PEG-TNPs or PE-PEG-biotins showed a low extent of colocalization in peripheral vesicles with simultaneously internalized transferrin but a high extent of colocalization with cointernalized folate, mirroring the aforementioned results for proteins bound to long-chain saturated (di16:0) PE-PEG anchors.

To assess whether the early endocytic routing of PE-PEG–anchored anti-DNP antibody (maximum valency = 2) or streptavidin (maximum valency = 4) was affected by the potential of these proteins to bind to more than one lipid anchor molecule (Schwartz et al., 2005; Schwartz and Bangs, 2007), we

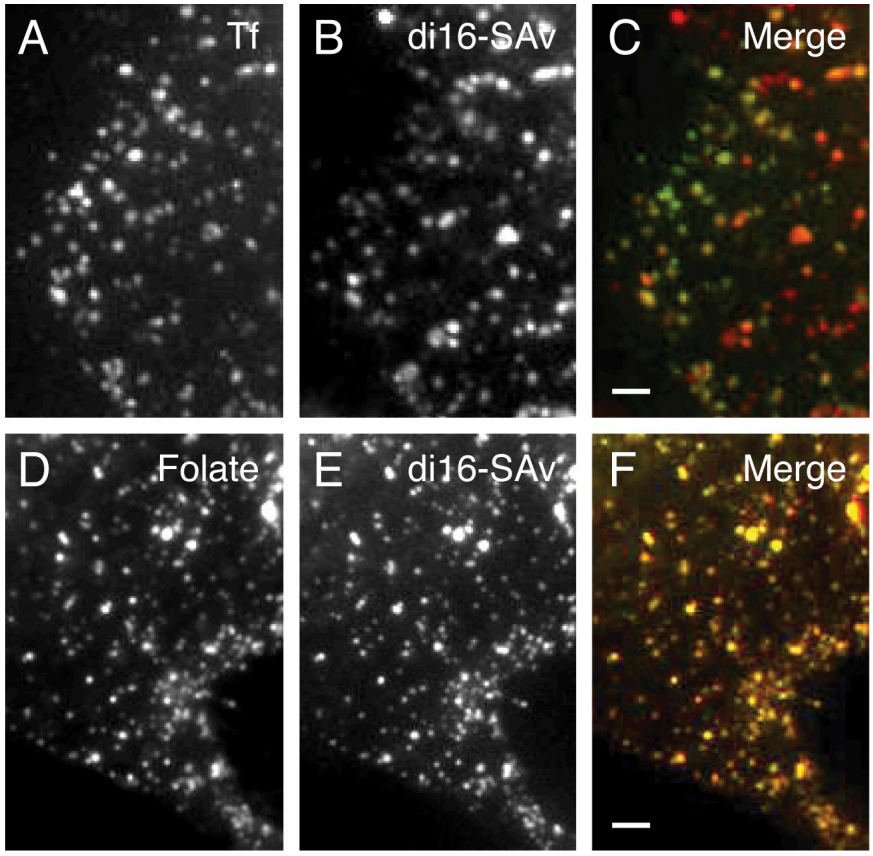

Figure 5. **di16:0PE-PEG–anchored streptavidin colocalizes only weakly with transferrin but strongly with the GPI-linked folate receptor in peripheral endocytic vesicles.** (A–F) Cells incorporating di16:0PE-PEGSS-biotin (structure shown in Fig. 1) were allowed to endocytose Alexa Fluor 555–labeled streptavidin (SAv; red in merged images) along with either Alexa Fluor 488–labeled transferrin (Tf; A–C) or fluorescein-labeled folate (D–F) for 10 min at 37°C and then rapidly chilled, stripped of surface-bound fluorescent labels, and fixed before microscopic observation. Other experimental details were as described in Materials and methods. Bars, 2 µm.

also examined the extent of colocalization of internalized transferrin and folate with fluorescent-labeled *E. coli* DHFR, a monomeric protein which binds methotrexate with 1:1 stoichiometry, in cells incorporating di12:0PE-PEG-methotrexate. As shown in Fig. 4 (B and C) and Fig. S1, PE-PEG–anchored DHFR, like lipid-anchored antibody or streptavidin, showed a high degree of colocalization with folate and a low degree of colocalization with transferrin in peripheral endocytic vesicles. These results indicate that the strong colocalization of PE-PEG–anchored proteins with the folate receptor but not with the transferrin receptor in peripheral endocytic structures does not require that the anchored protein bind to more than one lipid anchor.

To ensure that the aforementioned results could not be affected by potential remodeling of the probe acyl chains, we also performed analogous experiments using PE-PEG protein conjugates bearing nonhydrolyzable ether-linked hydrocarbon chains. Anti-DNP antibody anchored to membranes via either a disaturated (di-*O*-hexadecyl) or a diunsaturated (di-*O*-cis-9′-octadecenyl) diether PE-PEG-TNP also showed a high degree of colocalization with folate and a much lower extent of colocalization with transferrin in peripheral endocytic structures (Figs. 4, B and C; and 6, M–R). These findings indicate that the nature, and particularly the degree of saturation, of the hydrocarbon chains carried by the PE moiety exerts at most a minor influence on the tendency of PE-PEG–anchored proteins to colocalize with GPI proteins and not with transferrin in peripheral endocytic vesicles. Confocal microscopy showed that anti-DNP antibody anchored to short-chain (di12:0) or unsaturated (di16:1c) PE-PEGs colocalized strongly with transferrin in the central regions of the cell (unpublished data), which is similar to the aforementioned behavior for the same antibody anchored to di16:0PE-PEG.

In experiments analogous to those described in the previous paragraphs, we also compared the distributions of endocytosed bulk membrane lipid markers with those of simultaneously internalized transferrin or folate in peripheral endocytic vesicles. As illustrated in Fig. 7 (A–F), the membrane lipid marker DLMal-TMR (structure shown in Fig. 1) detectably labels a very high proportion of both the transferrin- and the folate-containing populations of peripheral vesicles. Similar results were observed using two other bulk membrane lipid markers, Bodipy-sphingomyelin (Fig. S2) and di12:0PE-PEG$_3$-fluorescein. Consistent with these observations, quantitative analysis (Fig. 7 M) indicates that DLMal-TMR colocalizes more extensively with internalized transferrin in peripheral endocytic vesicles than does folate, whereas it colocalizes more extensively with internalized folate than does transferrin.

The fluorescent probe DL1500-TMR (Fig. 1) corresponds to a PE-PEG anchor labeled at its distal terminus with a small fluorescent residue. Like the aforementioned bulk lipid markers, DL1500-TMR is found in a high proportion of both transferrin receptor– and folate receptor–containing peripheral vesicles (Fig. 7, G–L). Accordingly, quantitative analysis (Fig. 7 M) likewise shows that the protein-free PE-PEG marker is found in transferrin-positive peripheral vesicles to a much greater extent than is labeled folate and in folate-positive vesicles to a much greater extent than is labeled transferrin. Thus, the peripheral

localization of the protein-free PE-PEG marker resembles more closely the distribution of a bulk lipid marker than that of the GPI-anchored folate receptor (or of PE-PEG–anchored proteins; Fig. 4, B and C), although the PE-PEG marker may colocalize slightly more strongly with the folate receptor than does the bulk lipid marker (Fig. 7 M).

Modulation of different endocytic pathways affects internalization of GPI- and PE-PEG–anchored proteins in a similar manner

The GEEC/CLIC pathway has been shown to be clathrin and dynamin independent and regulated by Arf1 and cdc42 but not by RhoA (Sabharanjak et al., 2002; Kumari and Mayor, 2008). To assess further whether endogenous GPI proteins and PE-PEG–anchored proteins are internalized by the same pathway, we compared how the rates of endocytosis of PE-PEG protein conjugates, folate, and transferrin are affected by treatments that modify the cellular activities of dynamin, Arf1, and RhoA. As shown in Fig. 8 A, the dynamin-inhibiting agent dynasore (Macia et al., 2006; Kirchhausen et al., 2008) strongly inhibited the uptake of transferrin but had no effect on that of folate, which is consistent with the previous finding that endocytosis via the GEEC/CLIC pathway is dynamin independent (Sabharanjak et al., 2002). Dynasore also had no effect on the internalization of anti-DNP antibody anchored to di16:0PE-PEG-TNP or of (monomeric/monovalent) DHFR anchored to di16:0PEG-methotrexate (Fig. 8 A). A clathrin-independent, dynamin- and RhoA-dependent pathway distinct from the GEEC/CLIC pathway (Lamaze et al., 2001) has been reported to mediate internalization of the interleukin-2 receptor β subunit but not of GPI-anchored proteins in CHO cells (Sabharanjak et al., 2002). Consistent with our observation that inhibition of dynamin failed to affect the uptake of either folate or PE-PEG–anchored anti-DNP antibody, the internalization of both markers was also unaffected by expression of a dominant-negative mutant of RhoA (unpublished data).

Expression of a dominant-negative (T31N) form of Arf1 strongly inhibited the internalization of folate and of PE-PEG–anchored anti-DNP antibody but did not affect the uptake of transferrin (Fig. 8 B). Expression of a small hairpin RNA (shRNA) directed against Arf1 (Volpicelli-Daley et al., 2005) likewise differentially affected the uptake of these markers in a very similar pattern, whereas expression of a control shRNA directed against Arf3 did not significantly alter the uptake of any of these species (Fig. 8 C). Conversely, expression of a constitutively active (Q71L) form of Arf1 markedly stimulated the uptake of both folate and PE-PEG–anchored antibody (Fig. 8 D). Expression of activated Arf1 slightly reduced the uptake of transferrin, possibly reflecting compensatory regulatory interactions between the clathrin-mediated and other endocytic pathways (Damke et al., 1995). The observed effects of mutant Arf1 species and of Arf1 knockdown on the uptake of transferrin and folate agree well with those reported in a previous study (Kumari and Mayor, 2008), which also showed that the effects of Arf1 modulation on endocytosis via the GEEC/CLIC pathway are not mediated through effects on secretory trafficking. Thus, endocytosis of artificially lipid-anchored proteins responds to perturbations of the activities of dynamin, Arf1 (using several different treatments), and RhoA in a manner very similar to the observed effects of these perturbations on internalization of the folate receptor.

Inhibition of dynamin and modulation of Arf1 activity affected cellular uptake of the bulk membrane lipid marker DLMal-TMR in a pattern distinct from those observed for both transferrin and lipid-anchored proteins. Dynasore strongly reduced the cellular uptake of the lipid marker, which is in contrast to its minimal effects on the uptake of lipid-anchored proteins (Fig. 8 A). Expression of dominant-active Arf1 (Fig. 8 B) or of anti-Arf1 shRNA but not of a control anti-Arf3 shRNA (Fig. 8 C) also substantially reduced the uptake of DLMal-TMR while (as already noted) causing no significant inhibition of transferrin uptake. The observed sensitivity of bulk lipid uptake to inhibition of either dynamin or Arf1 is consistent with the conclusion from our colocalization experiments that bulk membrane lipids are endocytosed to significant extents both by clathrin-mediated endocytosis and by the GEEC/CLIC pathway in CHO cells. Also consistent with this conclusion, uptake of DLMal-TMR is slightly stimulated (by roughly 20%) in cells expressing constitutively activated (Q71L) Arf1 (Fig. 8 D), which is an effect intermediate between the mild inhibition of transferrin uptake and the strong stimulation of internalization of lipid-anchored proteins (folate receptor and PE-PEG–anchored anti-DNP antibody) that are observed under the same conditions.

As shown in Fig. 8, internalization of the fluorescent-labeled PE-PEG DL1500-TMR (structure shown in Fig. 1) was altered in a manner comparable with that observed for the bulk lipid marker DLMal-TMR in cells treated with dynasore (Fig. 8 A) or expressing dominant-negative or constitutively activated forms of Arf1 (Fig. 8, B and D). From these results and from the colocalization results presented earlier, it appears that the simple presence of the PEG linker is not sufficient to shift the endocytic behavior of a labeled PE-PEG (degree of colocalization with different markers and response to various modulators of endocytic pathways) from a bulk lipid-like pattern to the distinct pattern observed for GPI- or PE-PEG–anchored proteins. Instead, the presence of a tethered protein moiety (although not of a specific protein sequence or structure) appears to be a key requirement for PE-PEG–based conjugates to be internalized preferentially via the GEEC/CLIC pathway.

Discussion

The results obtained in this study provide several significant insights into the mechanism or mechanisms by which GPI-anchored proteins are readily internalized via the GEEC/CLIC pathway while exhibiting negligible uptake via clathrin-coated endocytosis in mammalian cells. First, this preferential endocytic routing clearly does not require specific structural elements of the complex GPI polar head group, ruling out any obligatory role for a putative GPI anchor–binding protein in the uptake of GPI proteins via the GEEC/CLIC pathway. Second, recruitment of lipid-anchored exofacial proteins into the GEEC/CLIC pathway does not require that the anchor carry long, saturated hydrocarbon chains like those found on many naturally occurring GPI

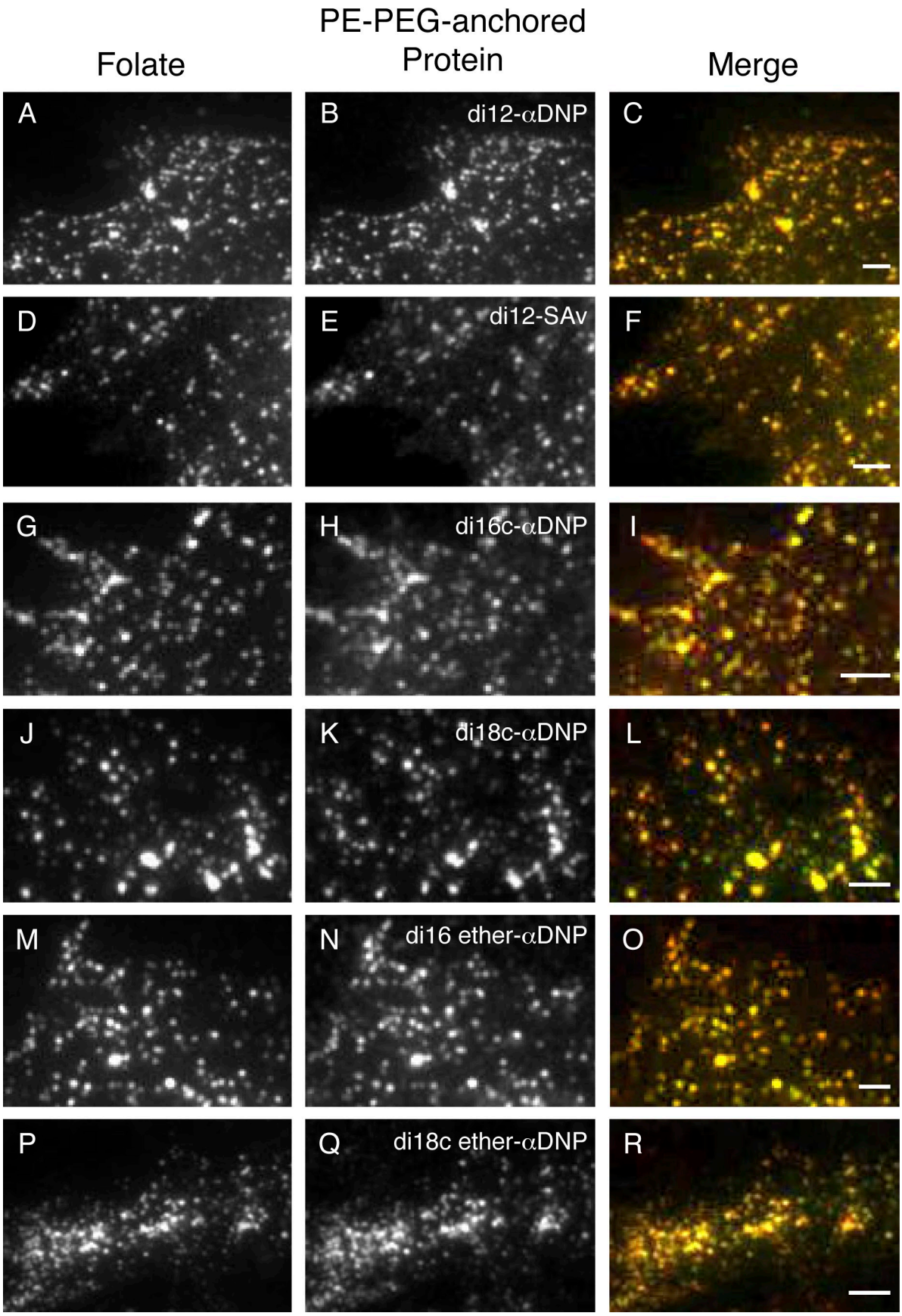

Figure 6. **Proteins anchored to PE-PEG anchors with different hydrocarbon chain structures colocalize with the GPI-anchored folate receptor in peripheral endocytic vesicles.** (A–R) Cells incorporating the indicated diacyl/dialkyl–PE-PEG-TNP or –PE-PEG-biotinyl anchors were incubated for 10 min with Alexa

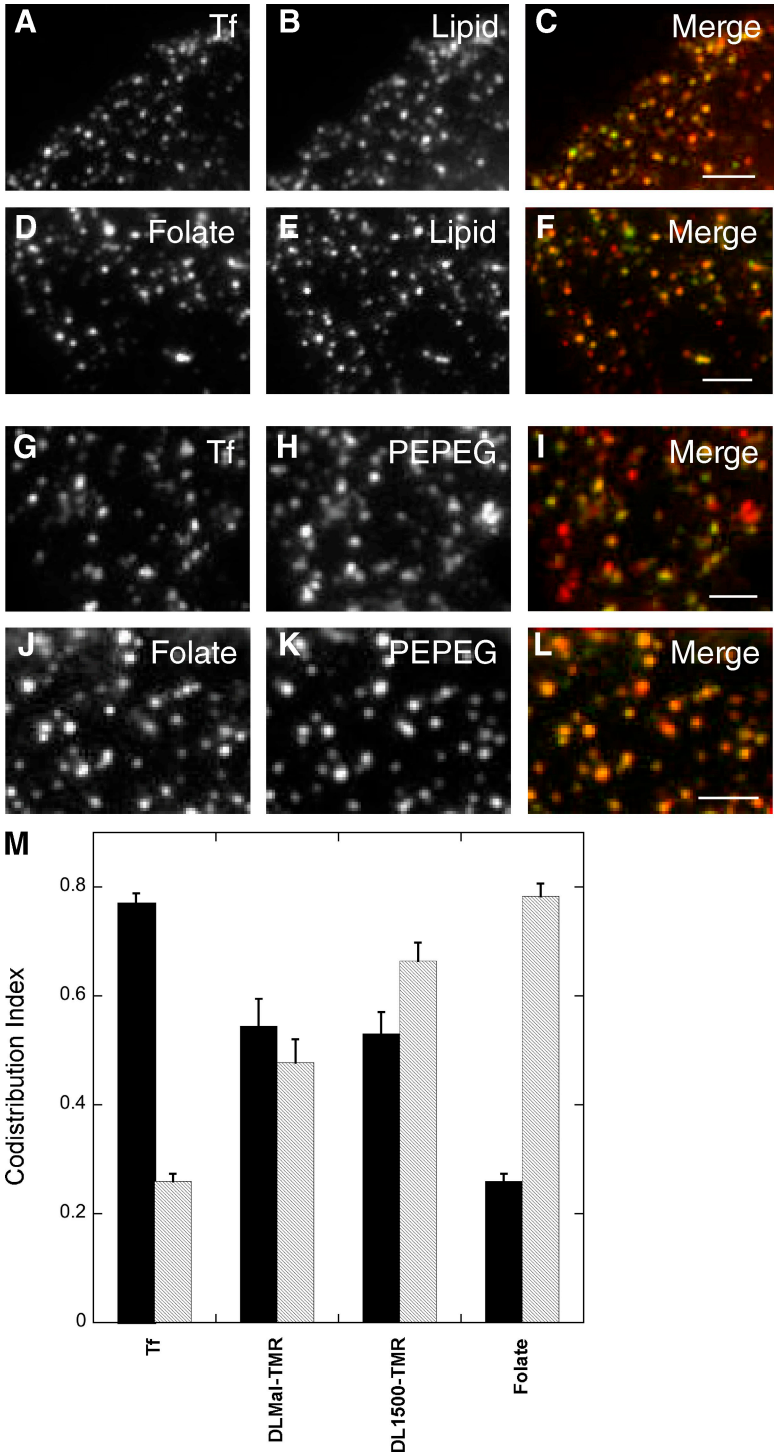

Figure 7. **A bulk lipid marker and a fluorescent PE-PEG label both transferrin- and folate-containing peripheral endocytic vesicles.** Cells were preincubated for 30 min at 4°C to incorporate DLMal-TMR or the fluorescent PE-PEG DL1500-TMR (structures shown in Fig. 1), fluorescent transferrin or folate was added, and the cells were rapidly warmed to 37°C. After 10 min, the cells were chilled, residual surface-bound fluorescent markers were removed, and the fixed cells were imaged by fluorescence microscopy. (A–F) Cells coincubated at 37°C with DLMal-TMR (lipid; red in merged images) and either Alexa Fluor 488–transferrin (Tf) or fluorescein-labeled folate. (G–L) Cells coincubated at 37°C with DL1500-TMR (PEPEG; red in merged images) and either Alexa Fluor 488–transferrin or fluorescein-labeled folate. The virtual absence of deep green vesicles (labeled by transferrin or folate only) illustrates the observation that essentially all transferrin- and folate-containing vesicles are also labeled to some extent by the lipid and PE-PEG markers. (M) Quantitation of the indexes of co-distribution of DLMal-TMR and DL1500-TMR with transferrin (solid bars) and folate (hatched bars). Values plotted represent the mean (±SEM) of determinations for 40–50 separate fields (all from distinct cells) in three to four independent experiments. The co-distribution indexes measured in parallel experiments for cointernalized Alexa Fluor 488– and Alexa Fluor 555–transferrin (Tf solid bar), fluorescein- and rhodamine-labeled folate (Folate hatched bar), and labeled folate and transferrin (Tf hatched bar and Folate solid bar) are shown for reference. Other experimental details are described in Materials and methods. Bars, 2 μm.

Fluor 555–anti-DNP antibody or Alex Fluor 555–streptavidin together with fluorescein-labeled folate (green in merged images) and then chilled, stripped of surface-bound fluorescent molecules, and fixed for fluorescence imaging. Anchor species and bound fluorescent proteins are designated as follows: di12-, di16c-, and d18c–α-DNP indicate anti-DNP antibody bound to di12:0-, di16:1c-, or di18:1cPE-PEG-TNP; di12-SAv indicates streptavidin bound to di12:0PE-PEGSS-biotin; di16 ether- and di18c ether–α-DNP indicate anti-DNP antibody bound to dihexadecyl– or di-cis-9′-octadecenyl–PE-PEG-TNP. Other experimental details were as described in Materials and methods. Bars, 2 μm.

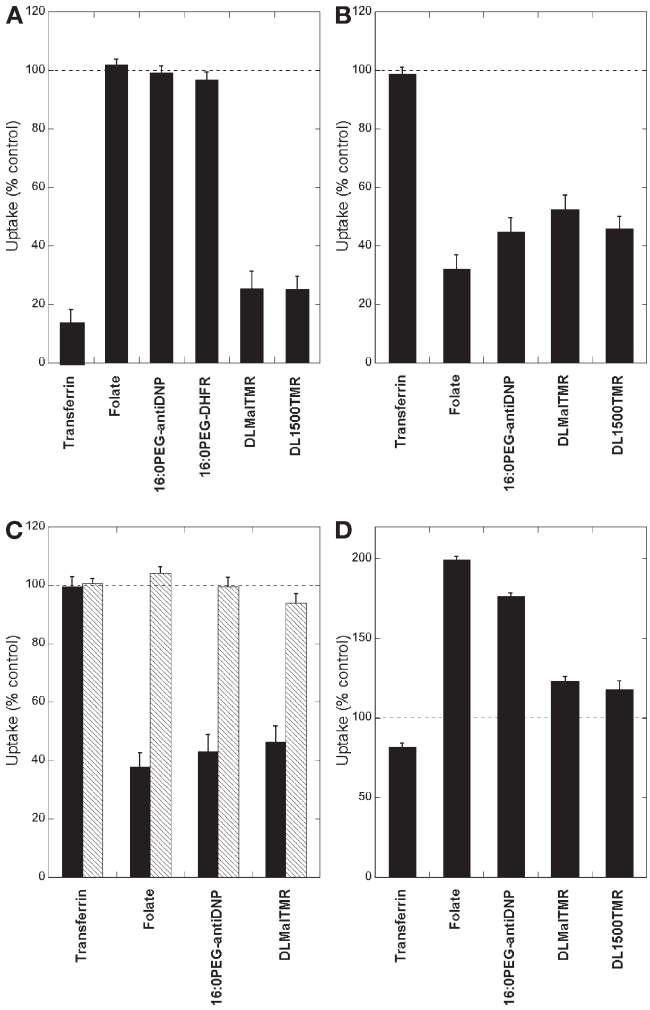

Figure 8. **Modulation of dynamin and Arf1 activities affects endocytosis of artificially lipid-anchored proteins in a manner very similar to that observed for GPI proteins.** Cells were allowed to internalize Alexa Fluor 555–transferrin, rhodamine-labeled folate, Alexa Fluor 555–labeled anti-DNP antibody (for cells incorporating di16:0PE-PEG-TNP), or DHFR (for cells incorporating di16:0PE-PEG-methotrexate), the bulk lipid marker DLMal-TMR, or the fluorescent PE-PEG DL1500-TMR (the latter two markers were preincorporated into the plasma membrane at 0°C) for 3 min at 37°C. The amount of internalized marker was then determined by microscopy after the removal of residual surface-associated markers and fixation as described in Materials and methods. Uptake of each fluorescence marker under the indicated treatments is expressed as a percentage of the level of marker internalization measured in parallel untreated control samples. Data values shown represent the mean (±SEM) determined from three to seven independent experiments. (A) Effects of 80 µM of the dynamin inhibitor dynasore preincubated with cells for 20 min. (B) Effects of transient expression of a dominant-negative (T31N) form of Arf1. (C) Effects of expression of shRNAs directed against Arf1 (solid bars) or against Arf3 as a negative control (hatched bars). (D) Effects of transient expression of a constitutively activated (Q71L) form of Arf1.

proteins (McConville and Ferguson, 1993; Maeda et al., 2007). This finding suggests that the ability of GPI proteins to associate with ordered-lipid microdomains does not determine their potential for recruitment into the GEEC/CLIC pathway. Finally, the presence of a bulky protein residue attached to the lipid anchor appears to be a key requirement for the preferential uptake of GPI proteins into the GEEC/CLIC pathway. This conclusion is based on our observations that artificial PE-PEG–anchored proteins closely resemble the GPI-linked folate receptor, and differ markedly from both simple lipid markers and PE-PEG molecules not bound to protein, in their distributions in peripheral endocytic vesicles and in the manner in which their uptake is affected by modulating the activities of dynamin and Arf1. Thus, it appears that the steric bulk of these lipid-anchored proteins is a critical determinant of their preferential routing into the GEEC/CLIC pathway in competition with, e.g., the coated pit pathway. Although steric interactions between membrane proteins have been hypothesized to influence their functional behavior in important ways (Grasberger et al., 1986), experimental indications of the significance of such effects have previously been limited mainly to observations of the kinetics of membrane protein diffusion (Frick et al., 2007). Our present results indicate that such steric interactions, although relatively rudimentary and nonspecific in nature, can exert important and even qualitative effects on the trafficking of some membrane proteins as well.

Our present results suggest that a significant fraction of the total endocytic flux of bulk plasma membrane lipids can be mediated via the GEEC/CLIC pathway. Fluorescent bulk lipid markers such as DLMal-TMR and Bodipy-sphingomyelin are readily observed in essentially all peripheral endocytic vesicles that contain the folate receptor, which is in agreement with the findings of Lundmark et al. (2008) using a different lipid marker, and the uptake of a bulk lipid marker is significantly modified by treatments that selectively modulate the activity of the GEEC/CLIC pathway. Based on the use of treatments that inhibit or activate particular endocytic pathways, precise quantitation of the relative contributions of different endocytic pathways to internalization of a given endocytic marker is complicated by the regulatory interactions that can occur between different pathways (Damke et al., 1995). Nonetheless, our results suggest that the coated pit pathway also mediates a substantial fraction of the overall endocytic flux of bulk membrane lipids, which is in agreement with previous conclusions (Puri et al., 2001; Sabharanjak et al., 2002). Our findings agree only partially with those of a previous study in which Bodipy-sphingomyelin was detected in transferrin- but not in folate-containing peripheral endocytic vesicles (Sabharanjak et al., 2002). This apparent discrepancy may reflect a quantitative rather than a qualitative difference (based on, e.g., different sensitivities of detection of the lipid markers). However, our findings agree with the key conclusion of Sabharanjak et al. (2002) that GPI proteins show important differences from bulk lipid markers in their overall endocytic behavior.

How can very simple, nonspecific features of the structures of exofacially lipid-anchored proteins, notably (as we have shown in this study) the steric bulk of the tethered protein moiety, allow these species to be taken up readily via the GEEC/CLIC pathway and not in parallel via the clathrin-mediated endocytic pathway? We suggest that the answer may lie at least partly in an ability of coated pits, as they concentrate their preferred membrane protein cargoes, to create highly crowded environments (at least at their extracytoplasmic faces) that tend to exclude membrane proteins lacking positive signals for recruitment to these structures. In the simplest model based on this proposal, the GEEC/CLIC pathway would serve as a simple

default/bulk process for uptake of lipid-bound proteins present in the exofacial leaflet of the plasma membrane, except in cases in which such proteins associate with other membrane proteins that recruit them to alternative endocytic pathways.

The aforementioned minimal model, although it appears broadly compatible with our present findings, may not accommodate all previously reported observations. Most notably, Sabharanjak et al. (2002) found that a chimeric protein, in which the normal GPI anchor of the folate receptor was replaced by an Fc-γ receptor transmembrane domain and the cytoplasmic sequence of the low density lipoprotein receptor, was internalized into transferrin-containing peripheral endocytic structures and not into GEEC/CLIC structures, even when the cytoplasmic sequence of the chimeric protein incorporated mutations that impair clathrin-mediated endocytosis of the native low density lipoprotein receptor. This result suggests that internalization of transmembrane proteins by the GEEC/CLIC pathway may require some form of positive targeting information, and it underscores the need for further investigation to confirm whether preferential internalization of membrane proteins via the GEEC/CLIC pathway requires specific sequence/structural/topological information or, conversely, rests purely on an absence of signals for endocytosis by other mechanisms. In this regard, we note that our finding that very rudimentary structural determinants dictate the preferential uptake of (exofacial) lipid-anchored proteins via the GEEC/CLIC pathway does not inherently imply that entry of such proteins into this pathway is purely nonspecific or unregulated. The diffusion and the distributions of both endogenous GPI proteins and artificially lipid-anchored proteins on the cell surface have been shown to be modulated by the cortical actin cytoskeleton and to depend on the presence of the bulky tethered protein moiety (Discher et al., 1994; Friedrichson and Kurzchalia, 1998; Varma and Mayor, 1998; Fujiwara et al., 2002; Nakada et al., 2003; Sharma et al., 2004; Wilson et al., 2004; Chadda et al., 2007; Goswami et al., 2008). Given our limited current understanding of the mechanistic bases for such phenomena, we cannot exclude that related mechanisms could function to recruit or to select lipid-anchored exofacial proteins as cargo for the GEEC/CLIC pathway, albeit without requiring recognition of specific sequence/structural motifs in the anchored species or their association with ordered-lipid microdomains.

Materials and methods

Materials

Transferrin and streptavidin (Sigma-Aldrich) and rabbit polyclonal anti-DNP IgG (Invitrogen) were labeled with Alexa Fluor 488– or Alexa Fluor 555–succinimidyl ester (Invitrogen) as per the manufacturer's instructions. *E. coli* DHFR, expressed from a plasmid constructed by inserting the complete coding sequence of the protein between the NdeI and BamHI sites of pMAL-p4X (New England Biolabs, Inc.), was purified from *E. coli* by affinity chromatography on methotrexate-Sepharose (Ghosh et al., 2008) and labeled with Alexa Fluor 555–succinimidyl ester. Fluorescein-labeled folate was originally obtained as a gift from S. Mayor (National Centre for Biological Sciences, Bangalore, India) and later synthesized by the method of McAlinden et al. (1991), as was its rhodamine-labeled analogue. All common chemicals were reagent grade or better.

Syntheses of PE-PEG-TNPs

α,ω-Diamino-PEG1500 (Fig. S3, species 1; Zalipsky et al., 1983) was reacted with 1 equivalent of Boc-ON (Itoh et al., 1975). The reaction products were extracted from 0.1 M aqueous $NaHCO_3$, pH 8.5, into 5× 1 vol CH_2Cl_2, combined with 2 equivalents of acetic acid, dried, redissolved in water, and fractionated on SP-Sephadex C-50 (GE Healthcare), eluting with a gradient of 0–20 mM NaCl. The pure mono-Boc–protected product was reacted overnight with 5 equivalents of succinic anhydride in 1:1 acetone/0.3 M $NaHCO_3$, pH 8.5, which was then acidified with acetic acid and extracted with 4× 1 vol CH_2Cl_2 to yield α-BocNH-ω-*N*-succinyl-PEG1500 (Fig. S3, species 2). This species was reacted overnight with 1.1 equivalents of dicyclohexylcarbodiimide (DCC) and 1.5 equivalents of *N*-hydroxysuccinimide (NHS) in dry 1:1 dimethylformamide (DMF)/CH_2Cl_2 and then with 1 equivalent of PE (extensively dried in vacuo) in dry $CHCl_3$/DMF containing 8 equivalents of diisopropylethylamine (DIEA) and 1.5 equivalents of trifluoroacetic acid (TFA) for 4 h at 40°C. The reaction mixture was diluted with 10 vol 1:1 methanol/0.1 M Mes, pH 6.0, and extracted four times with an equal volume of CH_2Cl_2. The pooled extracts were concentrated under vacuum, and the PE-PEG1500-NH-t-Boc was purified by preparative silica gel TLC in 50:16:6:6:3 CH_2Cl_2/acetone/CH_3COOH/CH_3OH/H_2O. The purified material was N-deprotected by treatment with HCl in dry chloroform at 0°C (Silvius and Gagné, 1984) and then reacted with 5 equivalents of trinitrobenzenesulfonic acid in 2:1 methanol/0.1 M $NaHCO_3$, pH 8.5, for 1 h at 25°C. After acidifying with acetic acid and adjusting to 1:1 (vol/vol) methanol/aqueous, the reaction products were extracted into 4× 1 vol CH_2Cl_2 and purified by TLC, in the manner just described for PE-PEG1500-NH-t-Boc conjugates, to yield PE-PEG-TNPs.

Synthesis of PE-PEG-methotrexates

Fmoc–glutamic acid α-t-butylester, preactivated overnight with 1.1 equivalents of DCC and 1.5 equivalents of NHS in dry 1:1 DMF/CH_2Cl_2, was reacted with 1 equivalent each of S-trityl (Trt) cysteamine (Glaser et al., 2004) and DIEA for 8 h at 22°C. The product was purified on a column of silica gel (eluting with 0.5–4% methanol), N-deprotected in 4:1 DMF/piperidine for 1 h at 22°C, and coupled to 1 equivalent of APA (preactivated for 1 h with 1 equivalent each of PyBOP and triethylamine) for 48 h in dimethyl sulfoxide. Purification by preparative TLC and S/O-deprotection in 97:3 TFA/triisopropylsilane for 3 h at 22°C yielded γ-cysteamidomethotrexate, which was coupled to ω-(maleimidobutyryl)-PE-PEG (Loughrey et al., 1990) in 3:1:1 methanol/CH_2Cl_2/0.5 M Hepes, pH 7.0 for 4 h at 22°C and purified by preparative TLC to yield PE-PEG-methotrexate.

Synthesis of DL1500-TMR

ω-Amino-PEG1500-di12:0PE was reacted with 1.2 equivalents each of TMR (5[6]-carboxytetramethylrhodamine) succinimidyl ester (Invitrogen) and triethylamine for 2 h in dry CH_2Cl_2 and then purified by TLC as described for PE-PEG-TNP.

Syntheses of PE-PEGSS-biotin species

S-MMT-mercaptopropionic acid, prepared from MMT chloride and 3-mercaptopropionic acid (Barlos et al., 1996), was activated with 1.1 equivalents of DCC and 1.5 equivalents of NHS in dry 1:1 DMF/CH_2Cl_2 for 12 h at 25°C and then reacted overnight with 1 equivalent of diamino-PEG1500 in 1:1 DMF/CH_2Cl_2. The monoderivatized PEG product (Fig. S4, species 3) was purified on SP-Sephadex C-50, eluting with 0–20 mM NaCl in 50% aqueous ethanol. The purified (S-MMT)-mercaptopropionyl-NH-PEG1500-NH_2 was N-succinylated and coupled to PE as described for PE-PEG1500-NH-t-Boc and then S-deprotected using 1% TFA and 3% triethylsilane in dry CH_2Cl_2 under argon for 45 min to yield ω-(mercaptopropionyl)amido-PE-PEG (Fig. S4, species 4). 4-S-Trt-mercaptobenzoic acid (Fig. S4, species 5; Kim, 2006), activated with 1.1 equivalents of DCC and 1.5 equivalents of NHS in 1:1 dry DMF/CH_2Cl_2, was added slowly to 10 equivalents of α,ω-diamino-PEG_3 in acetonitrile and then stirred for 18 h and concentrated under nitrogen. The residue was redissolved in ethyl acetate, washed with 3× 1 vol of 0.5 M Na_2CO_3, dried over Na_2SO_4, and concentrated under N_2. After drying under high vacuum, the products were purified by flash chromatography on silica gel 60, eluting with 0.1% triethylamine plus 3–10% methanol in CH_2Cl_2. The purified (Trt-mercaptobenzoyl)NH-PEG_3-NH_2 was reacted with biotin succinimidyl ester (DMF and 1 equivalent of DIEA for 5 h at 25°C), and the products were S-deprotected (97:3 TFA/triethylsilane for 1 h) and purified by flash chromatography to yield species 6 in Fig. S4. ω-(3-mercaptopropionyl-NH)-PE-PEGs (Fig. S4, species 4) were activated on the terminal sulfhydryl residue with 2 equivalents of carbomethoxylsulfenyl chloride for 12 h at 0°C in dry methanol; after adding 1 vol of 0.2 M Mes, pH 6.0, the products were extracted with 5× 1 vol CH_2Cl_2 and reacted under argon with 1 equivalent of 4-mercaptobenzoylamido-PEG_3-biotin (1:1 CH_2Cl_2/methanol for 12 h at 25°C). The PE-PEGSS-biotin product was purified as described for PE-PEG-TNPs.

Syntheses of fluorescent lipid markers

Bodipy-sphingomyelin was prepared by acylation of sphingosine phosphorylcholine with the succinimidyl ester of 5-(5,7-dimethyl-Bodipy)-1-pentanoic acid (Pagano et al., 2000). DLMal-TMR was prepared by derivatizing di12:0PE with 1.2 equivalents each of 4-maleimidobutyric acid succinimidyl ester (Sigma-Aldrich) and triethylamine in CH_2Cl_2 and then coupling glutathione to the recovered product and finally labeling the glutathionyl amino group with TMR succinimidyl ester. di12:0PE-PEG_3-fluorescein was synthesized by coupling di12:0PE to α-*N*-succinyl-ω-*N*-Boc-PEG_3, N-deprotecting the intermediate product with HCl/CH_2Cl_2, and labeling with the succinimidyl ester of 5(6)-carboxyfluorescein (Invitrogen).

Plasmids and cell transfection

PCR fragments encoding the complete coding sequences of the dominant-negative T17N and T19N forms of human cdc42 and RhoA, respectively, flanked at their 5′ and 3′ ends by EcoRI and BamHI sites and with GCCACC sequences preceding their initiator ATG codons, were prepared from plasmids provided by N. Lamarche (McGill University, Montreal, Quebec, Canada). The digested fragments were cloned between the EcoRI and BamHI sites of pcDNA3.1(−) (Invitrogen), and the resulting plasmids were digested with SpeI, treated with Klenow fragment, and religated to eliminate the remaining SpeI site. A PCR fragment comprising the internal ribosome entry site (nt 259–836) of encephalomyocarditis virus, flanked at the 5′ end by a BamHI restriction sequence and at the 3′ end by the sequence 5′-ACTAGTGACAAGGCATAACTTAAG-3′, was cloned into the aforementioned plasmids via their BamHI and AflII sites. A complete EGFP coding sequence (including the termination codon but omitting the initiator ATG) was finally cloned between the SpeI and AflII sites of the resulting plasmids to produce the bicistronic plasmids pc(cdc42[T17N]/GFP) and pc(RhoA[T19N]/GFP). Analogous bicistronic plasmids encoding the dominant-negative (T31N) and constitutively activated (Q71L) forms of human Arf1 along with EGFP were prepared similarly, using as the PCR template a pOCT-based plasmid incorporating the human Arf1 coding sequence (Open Biosystems) and introducing the appropriate mutations using a QuikChange II mutagenesis kit (VWR International). All constructs were verified by sequencing. Plasmids encoding shRNAs directed against Arf1 and -3 (Volpicelli-Daley et al., 2005) were provided by R. Kahn (Emory University, Atlanta, GA). Cells were transfected with plasmids using Fugene 6 (Roche) according to manufacturer's instructions 24–36 h before analysis of uptake of endocytic markers. For experiments in which cells were transfected with plasmids encoding mutant proteins or shRNAs, transfected cells were identified via expression of GFP encoded either in the second open reading frame of a bicistronic plasmid (mutant forms of Arf1 or RhoA) or by a separate, cotransfected plasmid (for anti-Arf1 and -Arf3 shRNAs, using a 4:1 molar ratio of shRNA- to GFP-encoding plasmid for transfection).

Incorporation of PE-PEGs into CHO cells

FRαTb-1 cells, a CHO cell-derived line stably coexpressing the GPI-anchored human folate receptor and human transferrin receptor (provided by S. Mayor; Mayor et al., 1998), were cultured to 40–70% confluency in folate-free Ham's F12 medium containing 10% dialyzed serum on glass coverslips or glass-bottomed culture dishes precoated with 10 µg/ml fibronectin. Ligand-substituted PE-PEGs were incorporated into cells by two methods. In the first, PE-PEG samples (dried under a stream of nitrogen and then in vacuo from stock solutions in methylene chloride) were dispersed in 290 mM sucrose and 1 mM Hepes, pH 7.2, by incubating for 5 min at 37°C, bath sonicating for 5 min, and heating to 50°C for 5 min. Cell monolayers were washed four times at 37°C with Hanks' buffered saline solution supplemented with 25 mM Hepes, pH 7.2, (HBSS) and once with 290 mM sucrose, 1 mM $CaCl_2$, and 1 mM Hepes, pH 7.2, and then incubated at 37°C with the PE-PEG dispersions (freshly supplemented with $CaCl_2$ to 1 mM) for 5 min at a concentration of 5–10 µM for di12:0PE-PEG derivatives or for 90 min at a concentration of 25 µM for other PE-PEGs. In the second method, dispersions of PE-PEGs complexed to BSA, prepared using the method of Pagano et al. (2000), were incubated at 37°C in HBSS with cell monolayers (previously washed four times with HBSS) for 5 min using 5–10 µM di12:0PE-PEG or for 60–90 min using 25–50 µM of other PE-PEGs. After incorporation of PE-PEGs by either method, cells were washed four times with HBSS and postincubated for 1 h in serum-free medium (or HBSS for cells treated with PE-PEGSS-biotin) at 37°C. PE-PEGs incorporated into cells by either of the aforementioned methods showed comparable behavior in the assays discussed in the Results section, although the second method gave markedly higher incorporation of PE-PEGs with di18:1c or di18:1c ether chains. After binding of fluorescent protein markers to cells treated by these procedures (see next section), measurements of cell-associated fluorescence indicated that the levels of PE-PEG–anchored proteins incorporated into the cell membrane were comparable with or lower than the levels of expressed transferrin or folate receptors.

Uptake of endocytic markers

Except where otherwise indicated, to initiate endocytic uptake, fluorescent proteins and other endocytic markers were added at 37°C in HBSS to washed cell monolayers at the following concentrations: 40 µg/ml or 20 µg/ml for Alexa Fluor 488– or Alexa Fluor 555–labeled proteins, respectively, and 100 nM or 25 nM for fluorescein- or rhodamine-labeled folate, respectively. After incubation at 37°C for the indicated times, the cells were rapidly chilled to 4°C and stripped of surface-bound markers in the cold by incubating under the following conditions: for transferrin or fluorescent folic acid derivatives, four times for 15 min each in ascorbate buffer (160 mM sodium ascorbate, 40 mM ascorbic acid, 1 mM $CaCl_2$, and 1 mM $MgCl_2$, pH 4.5; Sabharanjak et al., 2002); for anti-DNP antibody, four times for 15 min each in ascorbate buffer containing 10 mM DNP-lysine; for streptavidin, five times for 10 min each in HBSS supplemented with 10 mM cysteine and adjusted to pH 8.5; and for DHFR, four times for 15 min each in HBSS containing 30 µM methotrexate. Cells were then fixed for 30 min on ice in phosphate-buffered saline containing 3% formaldehyde, washed with cold HBSS, and mounted in 10% Mowiol, 25% glycerol, and 2.5% DABCO (1,4-diazabicyclo[2.2.2]octane) in 0.2 M Tris, pH 8.5. Samples incubated with fluorescein-labeled markers were mounted in the same medium containing 10% DABCO after incubating with 10 µg/ml nigericin for 10 min at room temperature to collapse any transmembrane proton gradients.

For experiments to examine endocytosis of fluorescent lipid probes, cells were first labeled with the fluorescent lipids by incubating for 30 min at 4°C with 2.5–10 µM labeled lipid–BSA complexes (prepared as described in Pagano et al. [2000]) in HBSS and then washed four times with cold HBSS. After adding a second endocytic marker and rapidly warming and incubating for the indicated times at 37°C, the cells were rapidly cooled to 4°C, stripped to remove the surface-bound pool of the second marker, and fixed as described in the previous section. Surface-associated lipid probe was then removed by incubation with HBSS containing 5% defatted BSA (six times for 10 min each at 22°C). The cells were finally washed with HBSS and imaged immediately thereafter. Endocytosis of the fluorescent PE-PEG marker DL1500-TMR was examined by a similar procedure, initially incorporating the labeled PE-PEG into cells as described in the previous section for other di12:0PE-PEG species.

Fluorescence microscopy and image analysis

For quantitations of the extent and kinetics of label uptake, cells were examined on a fluorescence microscope (TE300; Nikon) with a 20× NA 0.45 Plan-Fluor objective. Total integrated fluorescence (corrected for the local background fluorescence measured from nearby cell-free areas) was determined for 60–100 cells (in at least 10 distinct fields) per treatment and for a comparable number of untreated control cells in each experiment. The mean background-corrected fluorescence per cell was then further corrected for the mean (background subtracted) time 0 fluorescence signal per cell, which was determined for a comparable number of cells in parallel control samples (incubated with label at 4°C rather than at 37°C and then processed as for cells incubated at 37°C and photographed under identical image acquisition conditions using paired phase-contrast images to localize the cell margins for the control samples). Confocal microscopy was performed using a confocal microscope (LSM 5 Pascal; Carl Zeiss, Inc.) with a 63× NA 1.45 objective lens and a pinhole setting of 1.0 µm.

For measurements of colocalization of different endocytic labels, fixed cells were imaged on a wide-field fluorescence microscope (IX18; Olympus) using a 60× NA 1.45 Plan-Apochromat objective. The extent of colocalization of different fluorescent markers in peripheral endocytic vesicles was quantitated using an object-based colocalization algorithm implemented in Matlab R2008a. Pairs of high magnification images obtained from fields on the periphery of cells labeled with two endocytic markers and typically containing 150–400 vesicles per field were first processed with a spatial bandpass filter, and local maxima (with peak intensities exceeding an appropriately assigned threshold) were then determined in each image to identify small vesicles. For each of the paired filtered images (A and B), the positions of the centroids of all peaks thus identified were then determined. For the position of each peak in image A, the intensities measured in image A versus image B were recorded; the same was performed for the position of each peak in image B. Two linear correlation coefficients were then calculated: r(A/B), based on the first dataset (peak intensities in image A vs. intensities measured at the corresponding positions in image B); and r(B/A), based on the second

dataset. The values of the two correlation coefficients were then averaged to yield the co-distribution index presented in Figs. 4 and 7 M. Similar results were obtained using a related analysis based on the integrated intensities rather than the peak intensities for maxima identified in the paired images.

Online supplemental material

Fig. S1 illustrates the low degree of colocalization between internalized transferrin and *E. coli* DHFR bound to di16:0PE-PEG-methotrexate and the high degree of colocalization observed between internalized DHFR and folate under the same conditions. Fig. S2 illustrates the observation that early endocytic vesicles containing either transferrin or folate are extensively colabeled by Bodipy-sphingomyelin in cells allowed to internalize transferrin or folate and the fluorescent sphingomyelin marker simultaneously. Figs. S3 and S4 show diagrammatically the synthetic schemes followed to prepare PE-PEG-TNPs and PE-PEGSS-biotins, respectively. Online supplemental material is available at http://www.jcb.org/cgi/content/full/jcb.200903102/DC1.

We thank Dr. Claire Brown of the Imaging Facility for valuable technical discussions and assistance. Wide-field microscopic images for this project were taken at the McGill Life Sciences Complex Imaging Facility, which was established with the financial support of the Canada Foundation for Innovation.

This research was supported by an operating grant from the Canadian Institutes of Health Research (CIHR) to J.R. Silvius. P. Bhagatji was supported in part by graduate fellowship awards from the Chemical Biology Strategic Training Initiative of the CIHR and from the McGill University Faculty of Medicine. M. Refaei was supported by graduate fellowship awards from the CIHR and from the McGill University Faculty of Medicine.

Submitted: 18 March 2009
Accepted: 14 July 2009

References

Barlos, K., D. Gatos, O. Hatzi, N. Koch, and S. Koutsogianni. 1996. Synthesis of the very acid-sensitive Fmoc-Cys(Mmt)-OH and its application in solid-phase peptide synthesis. *Int. J. Pept. Protein Res.* 47:148–153.

Barr, D.J., A.G. Ostermeyer-Fay, R.A. Matundan, and D.A. Brown. 2008. Clathrin-independent endocytosis of ErbB2 in geldanamycin-treated human breast cancer cells. *J. Cell Sci.* 121:3155–3166.

Bonazzi, M., S. Spanò, G. Turacchio, C. Cericola, C. Valente, A. Colanzi, H.S. Kweon, V.W. Hsu, E.V. Polishchuck, R.S. Polishchuck, et al. 2005. CtBP3/BARS drives membrane fission in dynamin-independent transport pathways. *Nat. Cell Biol.* 7:570–580.

Chadda, R., M.T. Howes, S.J. Plowman, J.F. Hancock, R.G. Parton, and S. Mayor. 2007. Cholesterol-sensitive Cdc42 activation regulates actin polymerization for endocytosis via the GEEC pathway. *Traffic.* 8:702–717.

Cheng, Z.J., R.D. Singh, D.K. Sharma, E.L. Holicky, K. Hanada, D.L. Marks, and R.E. Pagano. 2006. Distinct mechanisms of clathrin-independent endocytosis have unique sphingolipid requirements. *Mol. Biol. Cell.* 17:3197–3210.

Damke, H., T. Baba, A.M. van der Bliek, and S.L. Schmid. 1995. Clathrin-independent pinocytosis is induced in cells overexpressing a temperature-sensitive mutant of dynamin. *J. Cell Biol.* 131:69–80.

Discher, D.E., N. Mohandas, and E.A. Evans. 1994. Molecular maps of red cell deformation: hidden elasticity and in situ connectivity. *Science.* 266:1032–1035.

Donaldson, J.G., N. Porat-Shliom, and L.A. Cohen. 2009. Clathrin-independent endocytosis: a unique platform for cell signaling and PM remodeling. *Cell. Signal.* 21:1–6.

Dunn, K.W., T.E. McGraw, and F.R. Maxfield. 1989. Iterative fractionation of recycling receptors from lysosomally destined ligands in an early sorting endosome. *J. Cell Biol.* 109:3303–3314.

Eyster, C.A., J.D. Higginson, R. Huebner, N. Porat-Shliom, R. Weigert, W.W. Wu, R.-F. Shen, and J.G. Donaldson. 2009. Discovery of new cargo proteins that enter cells through clathrin-independent endocytosis. *Traffic.* 10:590–599.

Fivaz, M., F. Vilbois, S. Thurnheer, C. Pasquali, L. Abrami, P.E. Bickel, R.G. Parton, and F.G. van der Goot. 2002. Differential sorting and fate of endocytosed GPI-anchored proteins. *EMBO J.* 21:3989–4000.

Frick, M., K. Schmidt, and B.J. Nichols. 2007. Modulation of lateral diffusion in the plasma membrane by protein density. *Curr. Biol.* 17:462–467.

Friedrichson, T., and T.V. Kurzchalia. 1998. Microdomains of GPI-anchored proteins in living cells revealed by crosslinking. *Nature.* 394:802–805.

Fujiwara, T., K. Ritchie, H. Murakoshi, K. Jacobson, and A. Kusumi. 2002. Phospholipids undergo hop diffusion in compartmentalized cell membrane. *J. Cell Biol.* 157:1071–1081.

Gauthier, N.C., P. Monzo, V. Kaddai, A. Doye, V. Ricci, and P. Boquet. 2005. *Helicobacter pylori* VacA cytotoxin: a probe for a clathrin-independent and Cdc42-dependent pinocytic pathway routed to late endosomes. *Mol. Biol. Cell.* 16:4852–4866.

Ghosh, P., J. Cheng, T.-F. Chou, Y. Jia, S. Avdulov, P.B. Bitterman, V.A. Polunovsky, and C.R. Wagner. 2008. Expression, purification and characterization of recombinant mouse translation initiation factor eIF4E as a dihydrofolate reductase (DHFR) fusion protein. *Protein Expr. Purif.* 60:132–139.

Glaser, M., H. Karlsen, M. Solbakken, J. Arukwe, F. Brady, S.K. Luthra, and A.I. Cuthbertson. 2004. ^{18}F-fluorothiols: a new approach to label peptides chemoselectively as potential tracers for positron emission tomography. *Bioconjug. Chem.* 15:1447–1453.

Goswami, D., K. Gowrishankar, S. Bilgrami, S. Ghosh, R. Raghupathy, R. Chadda, R. Vishwakarma, M. Rao, and S. Mayor. 2008. Nanoclusters of GPI-anchored proteins are formed by cortical actin-driven activity. *Cell.* 135:1085–1097.

Grasberger, B., A.P. Minton, C. DeLisi, and H. Metzger. 1986. Interaction between proteins localized in membranes. *Proc. Natl. Acad. Sci. USA.* 83:6258–6262.

Guha, A., V. Sriram, K.S. Krishnan, and S. Mayor. 2003. *Shibire* mutations reveal distinct dynamin-independent and -dependent endocytic pathways in primary cultures of *Drosophila* hemocytes. *J. Cell Sci.* 116:3373–3386.

Itoh, M., D. Hagiwara, and T. Kamiya. 1975. A new tert-butoxycarbonylating reagent, Z-tert-butyloxycarbonyloxyimino-2-phenylacetonitrile. *Tetrahedron Lett.* 16:4393–4394.

Kalia, M., S. Kumari, R. Chadda, M.M. Hill, R.G. Parton, and S. Mayor. 2006. Arf6-independent GPI-anchored protein-enriched early endosomal compartments fuse with sorting endosomes via a Rab5/phosphatidylinositol-3′-kinase-dependent machinery. *Mol. Biol. Cell.* 17:3689–3704.

Kim, N. 2006. Synthesis and characterization of amphiphilicFe_4S_4-core dendrimers as protein models. PhD thesis. North Carolina State University, Raleigh, NC. 224 pp.

Kirchhausen, T., E. Macia, and H.E. Pelish. 2008. Use of dynasore, the small molecule inhibitor of dynamin, in the regulation of endocytosis. *Methods Enzymol.* 438:77–93.

Kirkham, M., and R.G. Parton. 2005. Clathrin-independent endocytosis: new insights into caveolae and non-caveolar lipid raft carriers. *Biochim. Biophys. Acta.* 1745:273–286.

Kirkham, M., A. Fujita, R. Chadda, S.J. Nixon, T.V. Kurzchalia, D.K. Sharma, R.E. Pagano, J.F. Hancock, S. Mayor, and R.G. Parton. 2005. Ultrastructural identification of uncoated caveolin-independent early endocytic vehicles. *J. Cell Biol.* 168:465–476.

Kumari, S., and S. Mayor. 2008. ARF1 is directly involved in dynamin-independent endocytosis. *Nat. Cell Biol.* 10:30–41.

Lamaze, C., A. Dujeancourt, T. Baba, C.G. Lo, A. Benmerah, and A. Dautry-Varsat. 2001. Interleukin 2 receptors and detergent-resistant membrane domains define a clathrin-independent endocytic pathway. *Mol. Cell.* 7:661–671.

Leckband, D.E., F.J. Schmitt, J.N. Israelachvili, and W. Knoll. 1994. Direct force measurements of specific and nonspecific protein interactions. *Biochemistry.* 33:4611–4624.

Loughrey, H.C., L.S. Choi, P.R. Cullis, and M.B. Bally. 1990. Optimized procedures for the coupling of proteins to liposomes. *J. Immunol. Methods.* 132:25–35.

Lundmark, R., G.J. Doherty, M.T. Howes, K. Cortese, Y. Vallis, R.G. Parton, and H.T. McMahon. 2008. The GTPase-activating protein GRAF1 regulates the CLIC/GEEC endocytic pathway. *Curr. Biol.* 18:1802–1808.

Macia, E., M. Ehrlich, R. Massol, E. Boucrot, C. Brunner, and T. Kirchhausen. 2006. Dynasore, a cell-permeable inhibitor of dynamin. *Dev. Cell.* 10:839–850.

Maeda, Y., Y. Tashima, T. Houjou, M. Fujita, T. Yoko-o, Y. Jigami, R. Taguchi, and T. Kinoshita. 2007. Fatty acid remodeling of GPI-anchored proteins is required for their raft association. *Mol. Biol. Cell.* 18:1497–1506.

Mayor, S., and R.E. Pagano. 2007. Pathways of clathrin-independent endocytosis. *Nat. Rev. Mol. Cell Biol.* 8:603–612.

Mayor, S., and H. Riezman. 2004. Sorting GPI-anchored proteins. *Nat. Rev. Mol. Cell Biol.* 5:110–120.

Mayor, S., K.G. Rothberg, and F.R. Maxfield. 1994. Sequestration of GPI-anchored proteins in caveolae triggered by cross-linking. *Science.* 264:1948–1951.

Mayor, S., S. Sabharanjak, and F.R. Maxfield. 1998. Cholesterol-dependent retention of GPI-anchored proteins in endosomes. *EMBO J.* 17:4626–4638.

McAlinden, T.P., J.B. Hynes, S.A. Patil, G.R. Westerhof, G. Jansen, J.H. Schornagel, S.S. Kerwar, and J.H. Freisheim. 1991. Synthesis and biological evaluation of a fluorescent analogue of folic acid. *Biochemistry.* 30:5674–5681.

McConville, M.J., and M.A. Ferguson. 1993. The structure, biosynthesis and function of glycosylated phosphatidylinositols in the parasitic protozoa and higher eukaryotes. *Biochem. J.* 294:305–324.

Nakada, C., K. Ritchie, Y. Oba, M. Nakamura, Y. Hotta, R. Iino, R.S. Kasai, K. Yamaguchi, T. Fujiwara, and A. Kusumi. 2003. Accumulation of anchored proteins forms membrane diffusion barriers during neuronal polarization. *Nat. Cell Biol.* 5:626–632.

Naslavsky, N., R. Weigert, and J.G. Donaldson. 2004. Characterization of a nonclathrin endocytic pathway: membrane cargo and lipid requirements. *Mol. Biol. Cell.* 15:3542–3552.

Pagano, R.E., R. Watanabe, C. Wheatley, and M. Dominguez. 2000. Applications of BODIPY-sphingolipid analogs to study lipid traffic and metabolism in cells. *Methods Enzymol.* 312:523–534.

Paulick, M.G., M.B. Forstner, J.T. Groves, and C.R. Bertozzi. 2007. A chemical approach to unraveling the biological function of the glycosylphosphatidylinositol anchor. *Proc. Natl. Acad. Sci. USA.* 104:20332–20337.

Pelkmans, L., T. Bürli, M. Zerial, and A. Helenius. 2004. Caveolin-stabilized membrane domains as multifunctional transport and sorting devices in endocytic membrane traffic. *Cell.* 118:767–780.

Puri, V., R. Watanabe, R.D. Singh, M. Dominguez, J.C. Brown, C.L. Wheatley, D.L. Marks, and R.E. Pagano. 2001. Clathrin-dependent and -independent internalization of plasma membrane sphingolipids initiates two Golgi targeting pathways. *J. Cell Biol.* 154:535–547.

Ricci, V., A. Galmiche, A. Doye, V.E. Necchi, E. Solcia, and P. Boquet. 2000. High cell sensitivity to *Helicobacter pylori* VacA toxin depends on a GPI-anchored protein and is not blocked by inhibition of the clathrin-mediated pathway of endocytosis. *Mol. Biol. Cell.* 11:3897–3909.

Sabharanjak, S., P. Sharma, R.G. Parton, and S. Mayor. 2002. GPI-anchored proteins are delivered to recycling endosomes via a distinct cdc42-regulated, clathrin-independent pinocytic pathway. *Dev. Cell.* 2:411–423.

Sandvig, K., M.L. Torgersen, H.A. Raa, and B. van Deurs. 2008. Clathrin-independent endocytosis: from nonexisting to an extreme degree of complexity. *Histochem. Cell Biol.* 129:267–276.

Schwartz, K.J., and J.D. Bangs. 2007. Regulation of protein trafficking by glycosylphosphatidylinositol valence in African trypanosomes. *J. Eukaryot. Microbiol.* 54:22–24.

Schwartz, K.J., R.F. Peck, N.N. Tazeh, and J.D. Bangs. 2005. GPI valence and the fate of secretory membrane proteins in African trypanosomes. *J. Cell Sci.* 118:5499–5511.

Sharma, P., S. Sabharanjak, and S. Mayor. 2002. Endocytosis of lipid rafts: an identity crisis. *Semin. Cell Dev. Biol.* 13:205–214.

Sharma, P., R. Varma, R.C. Sarasij, K. Ira, K. Gousset, G. Krishnamoorthy, M. Rao, and S. Mayor. 2004. Nanoscale organization of multiple GPI-anchored proteins in living cell membranes. *Cell.* 116:577–589.

Silvius, J.R., and J. Gagné. 1984. Lipid phase behavior and calcium-induced fusion of phosphatidylethanolamine-phosphatidylserine vesicles. Calorimetric and fusion studies. *Biochemistry.* 23:3232–3240.

Skretting, G., M.L. Torgersen, B. van Deurs, and K. Sandvig. 1999. Endocytic mechanisms responsible for uptake of GPI-linked diphtheria toxin receptor. *J. Cell Sci.* 112:3899–3909.

Varma, R., and S. Mayor. 1998. GPI-anchored proteins are organized in submicron domains at the cell surface. *Nature.* 394:798–801.

Volpicelli-Daley, L.A., Y. Li, C.J. Zhang, and R.A. Kahn. 2005. Isoform-selective effects of the depletion of ADP-ribosylation factors 1-5 on membrane traffic. *Mol. Biol. Cell.* 16:4495–4508.

Wang, T.-Y., R. Leventis, and J.R. Silvius. 2005. Artificially lipid-anchored proteins can elicit clustering-induced intracellular signaling events in Jurkat T-lymphocytes independent of lipid raft association. *J. Biol. Chem.* 280:22839–22846.

Wilson, B.S., S.L. Steinberg, K. Liederman, J.R. Pfeiffer, Z. Surviladze, J. Zhang, L.E. Samelson, L.H. Yang, P.G. Kotula, and J.M. Oliver. 2004. Markers for detergent-resistant lipid rafts occupy distinct and dynamic domains in native membranes. *Mol. Biol. Cell.* 15:2580–2592.

Zalipsky, S., C. Gilon, and A. Zilkha. 1983. Attachment of drugs to polyethylene glycols. *European Polymer Journal.* 19:1177–1183.